Available online at www.sciencedirect.com
SCIENCE DIRECT®
Microporous and Mesoporous Materials 57 (2003) 199–209
MICROPOROUS AND MESOPOROUS MATERIALS
www.elsevier.com/locate/micromeso

High loading of C_{60} in nanochannels of mesoporous MCM-41 materials

Chia-Hung Lee [a], Tien-Sung Lin [b,*], Hong-Ping Lin [c], Qi Zhao [c], Shang-Bin Liu [c], Chung-Yuan Mou [a,*]

[a] *Department of Chemistry, National Taiwan University, 1, Roosevelt Road, Section 4, Taipei 106, Taiwan*
[b] *Department of Chemistry, Washington University, St. Louis, MO 63130, USA*
[c] *Institute of Atomic and Molecular Sciences, Academia Sinica, Taipei 106, Taiwan*

Received 17 May 2002; accepted 18 October 2002

Abstract

Very high loadings of C_{60} and C_{60}^- anions in MCM-41 mesoporous materials have been achieved by modifying the channel surface with amino-functional group. Detailed physical properties of these mesoporous materials containing C_{60} were characterized by EPR, NMR, XRD, FTIR and UV–vis spectroscopic techniques. The surface area and pore size of mesoporous materials were further determined by N_2 adsorption–desorption isotherms. The mesopores of MCM-41 show sieving behavior in excluding the larger sized $C_{120}O$ while absorbing the smaller C_{60} as indicated in the EPR studies.

Keywords: MCM-41; C_{60}; $C_{120}O$; Sieving; EPR

1. Introduction

MCM-41 materials belong to a family of mesoporous silicates (M41S), which was disclosed by Mobil researchers [1,2]. The materials consists of hexagonal arrays of uniform 2–10 nanometer-sized cylindrical pores. The channel pores are created by using the self-assembly of silicates with surfactant as the templates and followed by calcinations of organic part. The wall surface of MCM-41 mesoporous materials can further be modified with proper functional groups, such as amino ($-NH_2$), thiol (–SH) and linear alkyl chains ($CH_3(CH_2)_n-$) [3–5]. These functional groups provide accessibility for anchoring other substrates, including transition metal ions and other big molecules, which allow one to attach other molecules of interest and to probe the structure, dynamics and chemical reactivity of confined molecules in the nanochannel pores of these mesoporous materials.

Recently, "single molecular chemistry" taking place in nanorestricted environments has caused much interest in chemical community [6]. Reactions in which molecules are spatially constrained could lead to many new fundamental understandings about the use of local environment to control

* Corresponding authors. Fax: +1-314-935-4481 (T.-S. Lin), +886-2-2366-0954 (C.-Y. Mou).
E-mail addresses: lin@wuchem.wustl.edu (T.-S. Lin), cymou@ms.cc.ntu.edu.tw (C.-Y. Mou).

1387-1811/02/$ - see front matter
PII: S1387-1811(02)00591-7

chemical reactions. For example, Turro recently described the photochemistry of dibenzyl ketones adsorbed on many zeolites [7]. The reaction pathway becomes much restricted due to constrained diffusion of the intermediate radical species.

Fullerene is a good electron and free radical scavenger. The free radical chemistry of C_{60} is important both in fundamental chemistry [8,9] and in medical applications [10]. However, radical reactions are rapid and difficult to control. Furthermore undesired side reactions often occur if the reactants are not in proximity. In an attempt to explore the free radical reactions of C_{60} in confined space to mimic the site-specific reactivity in biological system, we undertook the synthesis of C_{60} embedded in the nanochannels of MCM-41 materials. Previously, various "brute-force" methods were employed to incorporate C_{60} in mesoporous materials, such as vapor (sublimation) transport method [11–13], and adsorption by refluxing with a saturated solution of C_{60} [14,15]. However, the contents of C_{60} embedded in mesoporous materials obtained from these preparations were relative low, not more than 1%. [1] We shall demonstrate high concentration of C_{60} can be embedded in the channels of MCM-41 solids by surface modification with amino-functional group and other chemical consideration. These high loading of C_{60} in the surface modified MCM-41 solids allowed us to study the free radical reactions of C_{60} in aqueous solution by the EPR technique [16]. The study revealed the efficiency of free radical (hydroxyl and methyl radicals) attacks on C_{60} in a nanoreactor environment is higher than that in a non-restricted environment. The effect is attributed to the proximity of the free radical generating sites (from the Fenton reaction) and the scavenging sites (C_{60}) in the nanorestricted environment.

The composite of fullerene in mesoporous silica will be an interesting material for many chemical studies in the future. In general, one can investigate various aqueous chemistry of C_{60} unexplored before. Particularly interesting will be medical applications of the composite as free radical scavenger. In addition, the photoluminescence property of the confined C_{60} can also be studied [17].

2. Experimental

2.1. Materials and methods of preparations

Even though the van der Waals diameter of C_{60} is about 1.0 nm, which is smaller than the pore diameter of MCM-41 (2.7 nm), the hydrophobic and electron-poor C_{60} exhibits low affinity toward the surface of MCM-41 materials. It has been reported that C_{60} can react with a primary amine via an anion radical intermediate as follows [8,18,19]:

$$C_{60} + H_2NR \rightarrow [C_{60}^{\cdot -} \ldots H_2NR^{\cdot +}] \rightarrow 1,2\text{-H(NHR)}C_{60} \quad (1)$$

We would therefore expect a similar reaction to take place when the C_{60} solution is mixed with MCM-41–NH_2 to give MCM-41–NH–C_{60}H solids. The C_{60} functionalized MCM-41 solids would provide accessibility for anchoring other substrates, including transition metals ions, for many physical and chemical studies. Thus, the amino modification of the MCM-41 surface provides not only the binding sites for C_{60}, but also the hydrophilicity that enables us to study the free radical reaction of C_{60} in aqueous media. However, unlike the addition of isolated amine to C_{60} which could lead to $C_{60}H_6(NRR')_6$ [18], the geometric constraint of MCM-41–NH_2 would allow only a single –NH_2 to add onto C_{60} to form –NH–C_{60}H. Thus, we proceed the preparation by modifying the surface of MCM-41 with amino-functional groups to enhance the affinity toward C_{60}. The over-all methods of preparation consists of several steps: the preparation of MCM-41, surface

[1] Except the value reported in Ref. [14]: 20% of C_{60} by weight was incorporated in MCM-48 solids. This result is very different from that of Ref. [15] where the same method was employed but only 0.7% of C_{60} was reported. Note that the saturated C_{60} toluene solution is the limiting factor, which is about 1 mg/ml. Furthermore, 20% of C_{60} in the channel would lead to the intermolecular distance smaller than the van der Waals diameter of C_{60} if all the fullerenes are loaded inside the mesoporous in a linear array (see analysis given in Section 3.1). Thus, we have doubt about the analysis given in Ref. [14].

functionalization, and the covalent attachment of C_{60} to the surface functional group. Below we describe the details of our methods of preparation.

2.1.1. Synthesis of MCM-41

The MCM-41 was prepared according to a recipe given previously [3]. Briefly, 27.4 g of cetyltrimethylammonium bromide was fully dissolved in 240 g of water. 35.6 g of sodium silicate solution was added to the above mixture by constant stirring. 42 g of dilute sulfuric acid (1.2 M) was added slowly to the resulting mixture by pipette under stirring for 1 h at 32 °C, then hydrothermal at 100 °C for 2 days in a PTFE-lined autoclave. The final product was recovered by filtration, followed by washing with deionized water twice, dried at 100 °C and calcined at 540 °C for 8 h.

2.1.2. Synthesis of amino-modified MCM-41 (MCM-41–NH_2)

The synthesis of MCM-41 modified with amino-functional group has been reported previously [20]. The authors used less amount of silane (5.63 mmol of $NH_2(CH_2)_3Si(MeO)_3$ per gram of MCM-41) to modify the surface of MCM-41 at ambient temperature. The modification was reported to be mostly on the external surface. In order to increase the efficiency of modification, we used much more amount of silane (27.88 mmol of NH_2-$(CH_2)_3Si(MeO)_3$ per gram of MCM-41) to modify MCM-41 at higher temperature (110 °C). So both external surface and internal surface can be modified. The internal surface ($\approx$1000 m^2/g) of MCM-41 is much higher than external surface ($\approx$45 m^2/g), so $NH_2(CH_2)_3Si(MeO)_3$ is mostly modified on the internal surface of –OH groups.

Our reaction condition is as follows: 0.5 g of the calcined MCM-41 was placed in 100 ml toluene and stirred for 30 min 2.5 g of 3-aminopropyl trimethoxysilane (APTS) was added to the resulting mixture. The above reaction was allowed to run overnight at 110 °C. The solids were washed twice with pure toluene and acetone, filtered, and dried under vacuum. The washings were to ensure that the amino groups attached on the external surface were removed.

2.1.3. Binding of C_{60} and C_{60}^- on the amino-modified MCM-41 channels (MCM-41–NH–$C_{60}H$)

We prepared the C_{60} embedded in the nanochannels of MCM-41–NH_2 by introducing 0.4 g of amino-modified MCM-41 into 40 ml toluene solution containing high concentration of C_{60} (1 mg/ml). After the solution was under reflux overnight, the solids were washed twice with pure toluene and acetone, filtered, and dried under vacuum. From the data of elemental analysis (see Table 1), there is 0.018 mmol C_{60} bound on the surface per gram MCM-41–NH_2 that gives 1.21% for the calculated percentage of C_{60} binding on MCM-41–NH_2. These low loading samples inhibited us to perform many of the planned experiments, such as the study of free radical reactions of C_{60} embedded in mesoporous materials [16].

However, one may modify the hydrophobicity of C_{60} by one-electron reduction with mercury. Moreover, C_{60}^- is electron-rich and generally more reactive in electrophilic addition reaction. For example, KC_{60} is known to polymerize at low temperature [8,21], and bis(arene)chromium fullerides dimerize after electron transfer to C_{60} [22]. Furthermore, the solubility of C_{60}^- in organic solvents, such as THF, is much higher than that of neutral C_{60}. Thus, we employed fullerides as the starting material to increase the loadings of C_{60} in mesoporous materials.

The hydrophilic anion C_{60}^- species was prepared by mixing 0.2, 0.1, 0.05 or 0.15 mmol C_{60} with tetrahexyl ammonium bromide (the mole ratio of

Table 1
The amounts of C_{60} inside the MCM-41–NH_2 channels

	mmol of C_{60} per gram of sample	Number of C_{60}/$(nm)^2$	Average distance between C_{60} (nm)
MCM-41–NH–$C_{60}H$[a]	0.018	0.014	13
MCM-41–NH–$C_{60}H$[b]	0.074	0.059	3.1
MCM-41–NH–$C_{60}H$[c]	0.080	0.064	2.9
MCM-41–NH–$C_{60}H$[d]	0.089	0.071	2.6
MCM-41–NH–$C_{60}H$[e]	0.099	0.080	2.3

Refluxing of MCM-41–NH_2 with [b]0.2 mmol C_{60}, [c]0.1 mmol C_{60}, [d]0.05 mmol C_{60}, [e]0.15 mmol C_{60}, in 40 ml THF and three drops of Hg under nitrogen atmosphere.

[a] Refluxing C_{60} with MCM-41–NH_2 in toluene.

C_{60}/THAB = 0.2) in 40 ml THF and 2–3 drops Hg. The solution was heated and maintained at 80 °C for 3 h under nitrogen atmosphere [23]. The solution became dark red at the end of 3 h which is the characteristic color of C_{60}^- radical ions. Next we prepared the target material by mixing the above solution with 500 mg MCM-41–NH_2. After stirring the mixture for 12 h under nitrogen atmosphere, the solids were washed twice with toluene and acetone, filtered, and dried under vacuum. From the data of elemental analysis (Table 1), there is 0.074–0.099 mmol C_{60} bound on the surface per gram MCM-41–NH_2. The calculated percentage of C_{60} binding on MCM-41–NH_2 is 5.00–6.70%, which is almost a factor of 5.5 greater than the direct reaction of C_{60}/toluene with MCM-41–NH_2. The reaction of MCM-41 with APTS and the binding of C_{60}^- on MCM-41–NH_2 are summarized in Scheme 1.

The C_{60}^- anion bound on the surface of MCM-41–NH_2 could further react with oxygen according to the following reaction [24]:

$$C_{60}^- + O_2 \rightarrow C_{60} + O_2^- \quad (2)$$

Reaction (2) will proceed only if O_2^- is irreversibly removed from the system, presumably via proton or metal ion catalyzed disproportionation to peroxide or dioxygen [8]. Since the sample did not exhibit an EPR signal of C_{60}^- at room temperature, we would infer the sample most likely retained as neutral C_{60} or epoxide on the surface once it was exposed to the air. We designate the structure of C_{60} embedded in the mesoporous materials as MCM-41–NH–C_{60}H.

It should be noted if the nanostructured materials were uncalcined, it would be possible to solubilize C_{60} inside the nanochannels. Previously, we showed that C_{60} could be embedded into the interlayer of the hydrophobic phase of the layered double hydroxide with the help of surfactant molecules [25]. However, the unbound C_{60} would also be simultaneously removed with surfactants. In the present study, the surface modification leading to the covalent bonding of C_{60} is a necessary step so that the leachings in applications can be prevented.

2.2. Characterization techniques

The surface area and pore size was determined by N_2 adsorption–desorption isotherms obtained at 77 K on a Micrometric ASAP 2010 apparatus. The sample was out gassed at 300 °C for about 6 h in 10^{-3} Torr prior to adsorption. The pore size distribution curves were obtained from the analysis of the desorption portion of the isotherms using the Barrett–Joyner–Halenda method.

The structures of MCM-41, MCM-41–NH_2 and MCM-41–NH–C_{60}H solids were analyzed by X-ray powder diffraction (XRD) (Scintag X1 diffractometer, Cu Kα radiation at $\lambda = 0.154$ nm). FTIR measurements were recorded on a Nicolet 550 spectrometer using a KBr pellet. About 1 mg of sample was mixed with 300 mg of dried KBr and then pressed. The diffuse reflectance UV–vis spectra were measured with a Shimadzu UV-2101PC. Powdered samples were loaded in a quartz cell, and the spectra were collected in the 200–800 nm wavelength ranges against a standard.

$^1H \rightarrow {}^{13}C$ CP/MAS (cross polarization/magic angle spinning) NMR spectra were carried out on a Bruker MSL 500 spectrometer at room temper-

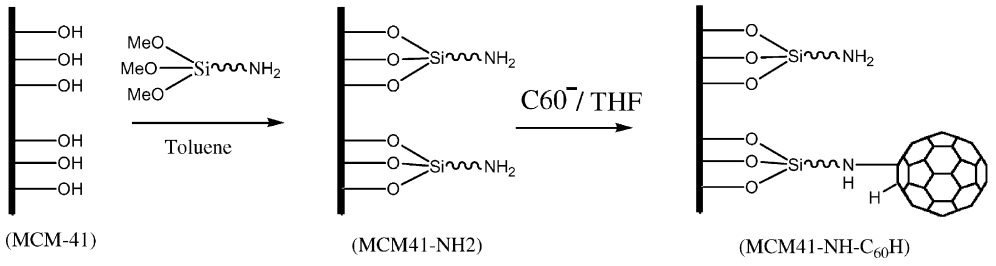

Scheme 1. Preparation scheme of MCM-41–NH_2 and MCM-41–NH–C_{60}H solids.

ature. The spectra were taken under the following conditions: ^{13}C frequency at 125.77 MHz, sample spinning rate at 6 kHz, pulse sequence with 5 ms contact time, recycle delay at 6 s, and signal average at 4000–8000 scans. Adamantane was used as the external reference.

We employed an X-band EPR spectrometer (Bruker ER300) for EPR measurements. A flat rectangular quartz sample cell (volume = 400 μl) was used to measure the EPR spectra of aqueous liquid mixtures. A quartz tubing of 4 mm OD was used for the solid sample. The spectrometer is equipped with a variable temperature set-up, which allows us to perform low temperature experiments (100 K to room temperature). Typical spectrometer settings are: microwave frequency: 9.74 GHz, microwave power: 1–2 mW, modulation amplitude: 1–5 G (depends on the line width), multiple scans were often required to obtain good signal/noise ratio. We used a solid sample of DPPH ($g = 2.0037$) as the standard for the g-value determination.

3. Results and discussion

3.1. Elemental analysis, surface area and pore size

The data of elemental analysis for five different samples are given in Table 1. There is 1.48 mmol of $-NH_2$ per gram MCM-41–NH_2. From the difference of carbon contents between MCM-41–NH_2 and MCM-41–NH–$C_{60}H$ samples, the calculated loadings of C_{60} are: 0.074–0.099 mmol C_{60} per gram MCM-41–NH–$C_{60}H$ for the loading of fulleride anion, and only 0.018 mmol for the neutral C_{60}. The difference is due to much higher solubility and affinity of C_{60}^- toward the amino-modified surface of MCM-41 solids as mentioned above.

The surface areas and pore diameters of MCM-41–NH_2 and MCM-41–NH–$C_{60}H$ in comparison with unmodified MCM-41 matrix are given in Table 2. We note that the surface area has been reduced from 1015 m^2/g in the unmodified MCM-41 to 753 m^2/g in the modified MCM-41–NH_2, a 25% reduction. The pore diameter of the mesoporous material has also been reduced from 2.7 to 1.7 nm after the $-O_3Si(CH_2)_3NH_2$ modification

Table 2
Surface area, pore diameter of MCM-41 solids

	Surface area (m^2/g)	Pore diameter (nm)
MCM-41	1015	2.7
MCM-41–NH_2	753	1.7
MCM-41–NH–$C_{60}H$[a]	636	1.7
MCM-41–NH–$C_{60}H$[b]	321–234	1.3–1.7

[a] Refluxing C_{60} with MCM-41–NH_2 in toluene.
[b] Refluxing C_{60}^- with MCM-41–NH_2 in THF under nitrogen atmosphere.

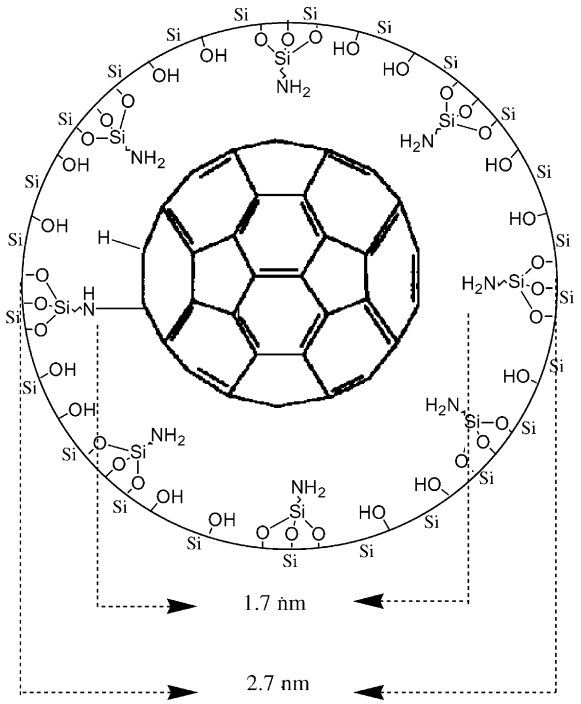

Diagram 1. C_{60} in the channel of MCM-41–NH_2.

(see Diagram 1). The reduction in the surface area and pore diameter indicates the amino groups are attached on the inner wall surface of the nanochannels. Reduction in these two parameters is further observed after the introduction of C_{60}^- in the samples: surface area is reduced to 321–234 m^2/g and pore diameter down to 1.3–1.7 nm. The drastic reduction of surface area in MCM-41–NH–$C_{60}H$ sample indicates that a good fraction of the surface area of the channel is now occupied by the bulky C_{60}. The pore diameter of 1.3–1.7 nm indicates an inhomogeneous distribution of substituted and

unsubstituted sites by C_{60}. However, we notice that the low loading of neutral C_{60} in MCM-41–NH–C_{60}H do not affect much on either the surface area (≈636 m^2/g) or pore diameter (≈1.7 nm).

From the elemental analysis and surface area determination, we find the effective modification of MCM-41 is 1.18 (number of $-NH_2/(nm)^2$), and that of C_{60} binding on MCM-41–NH_2 is 0.059–0.080 (number of $C_{60}/(nm)^2$). In terms of moles, the loading of C_{60} is much smaller than that of amino-functional group. This is reasonable since most of the amino groups are blocked from further attachment of C_{60} once one fullerene is attached (see Diagram 1).

We should point out the loading of C_{60} in MCM-41–NH_2 using the C_{60}^- route is extraordinarily high as illustrated in the following simple calculation. If all the C_{60} are loaded inside the mesopores in single file (i.e. in a linear array), the average distance between C_{60} molecules would be 3.1–2.3 nm, only 3.1–2.3 times greater than the close contact distance of 1.0 nm. Thus, we have an extraordinarily dense distribution of C_{60} in the confined space, which is very advantageous for other applications, such as free radical reactions of C_{60} in the nanochannel pore [16] and optical studies [17].

3.2. Spectroscopic characterization

3.2.1. FTIR

Fig. 1a shows the IR spectra of MCM-41 solids. In the amino-modified MCM-41 sample (Fig. 1b), the presence of APTS($-Si(CH_2)_3NH_2$) functional group on the wall surface is confirmed by the presence of the N–H (primary amine) bending vibration at 1550 cm^{-1}, and C–H stretching at 2944 cm^{-1}. The spectrum of MCM-41–NH–C_{60}H is given in Fig. 1c. We observed a drastic intensity decrease of the N–H bend at 1550 cm^{-1}, which is attributed to the conversion of primary amine to secondary amine after the binding with C_{60} (see band 1 and 2 in the expanded scale displayed in the inset). We should point out the N–H bending vibration of the secondary amine is normally very weak and usually not observable [26]. Furthermore, two peaks at 2950 and 2859 cm^{-1} are ascribed to C–H stretching on $-C_{60}$H moiety [27].

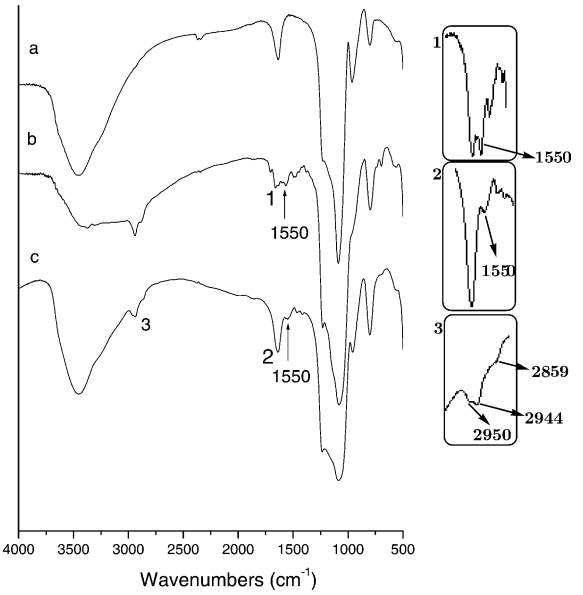

Fig. 1. IR spectra of (a) MCM-41, (b) MCM-41–NH2, and (c) MCM-41–NH–C_{60}H solids. The insets display the expanded scale of 1550 cm^{-1} band (#1 and #2), 2859, 2944 and 2950 cm^{-1} bands (#3).

3.2.2. X-ray diffraction

The siliceous MCM-41 gives a well-resolved XRD pattern as described by Beck et al. [1,2]. The XRD patterns of siliceous MCM-41, MCM-41–NH_2 and MCM-41–NH–C_{60}H are shown in Fig. 2a–c, respectively. The broadening and the reduction of intensity of (1 0 0) peak in MCM-41–NH_2 (Fig. 2b), resulting from the functionalization step, indicate some disorder of the meso-structure. After binding with C_{60} molecules, the value of the d_{100} peak remains the same (Fig. 2c). This indicates that C_{60} inside the channel of MCM-41–NH_2 does not damage the structure of MCM-41. The reduced intensity is probably due to the extraordinarily high loading which gives rise to lower spectral contrast.

3.2.3. Diffuse reflectance UV–vis spectra

Fig. 3a shows the UV–vis spectra of MCM-41 solids. In the amino-modified MCM-41 sample show the aminosilane absorption band at 300 nm (Fig. 3b) [28]. After binding with C_{60}, we observed the appearance of an intense long tail absorption band (Fig. 3c). Previously, it has been reported

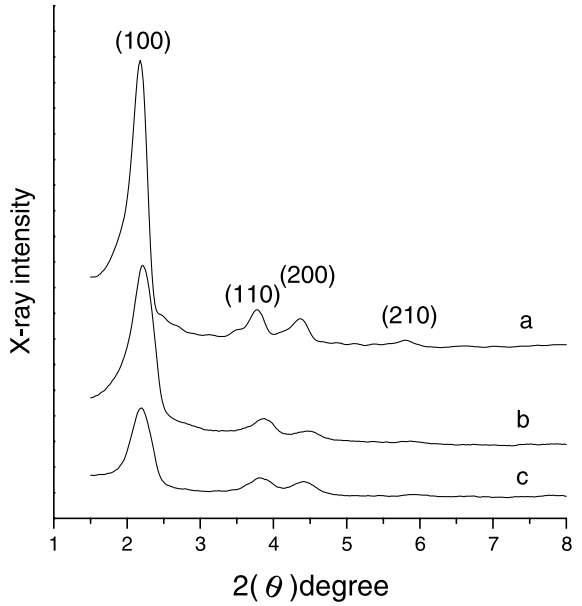

Fig. 2. XRD patterns of (a) MCM-41, (b) MCM-41–NH_2, and (c) MCM-41–NH–$C_{60}H$ solids. The reduced intensity in (c) may be due to the extraordinarily high density loading of C_{60}^-, which gives rise to lower spectral contrast.

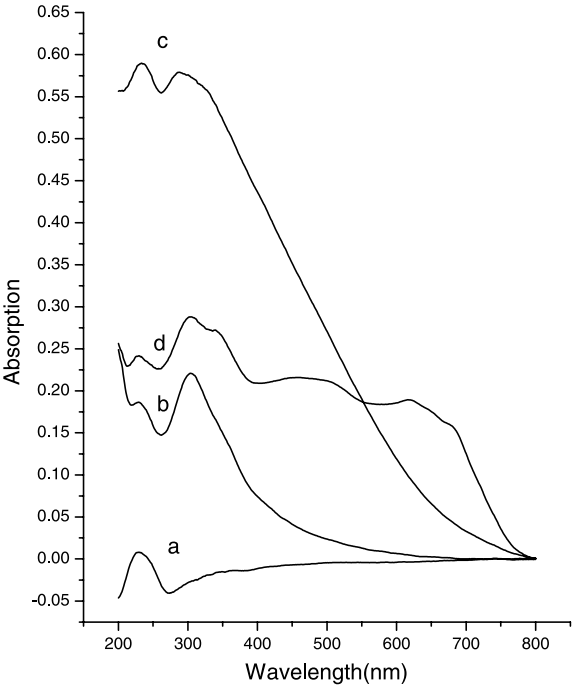

Fig. 3. Diffuse reflectance UV–vis spectra of the following solids: (a) MCM-41, (b) MCM-41–NH_2, (c) MCM-41–NH–$C_{60}H$, and (d) ground mixture of MCM-41–NH_2 and C_{60}.

that the saturation of one of the double bonds on C_{60} can give rise to a long tail band extended to 550 nm [29], thus we infer the C_{60} are bound to amino groups and form –$C_{60}H$ moiety. A similar long tail band was also observed in a homogeneous reaction mixture of C_{60} and 3-aminopropane [29], and in C_{60} molecules attached on silica surface [30]. Furthermore, if we physically ground MCM-41–NH_2 together with C_{60}, we observed only the characteristic absorption of C_{60}, but not the long tail band (Fig. 3d).

To further confirm amino-functional groups are indeed located inside the channels of MCM-41, we carried out a reaction of MCM-41–NH_2 with ninhydrin (see Scheme 2). It is well known that the reaction of ninhydrin with primary amines will produce Ruhemann's purple which should display the absorption bands at 405 and 570 nm [30,31]. However, ninhydrin cannot react with secondary amine. Fig. 4a displays the absorption spectrum of the mixture of MCM-41 solids and the ethanol solution of ninhydrin. There we observed an absorption band at 360 nm, which is attributed to the unreacted ninhydrin. On the other hand, we

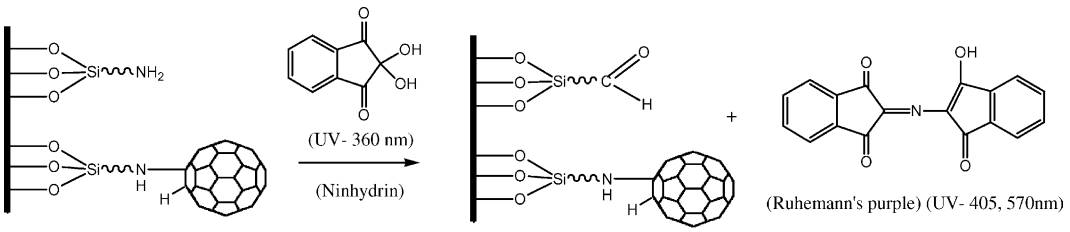

Scheme 2. The reaction of MCM-41–NH–$C_{60}H$ with ninhydrin.

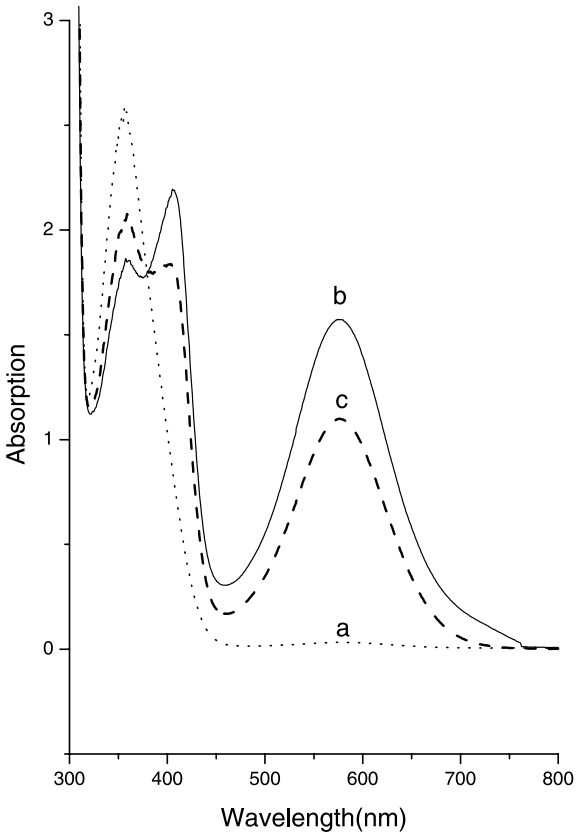

Fig. 4. Diffuse reflectance UV–vis spectra of the reaction product of ninhydrin with (a) MCM-41, (b) MCM-41–NH_2, and (c) MCM-41–NH–C_{60}H solids.

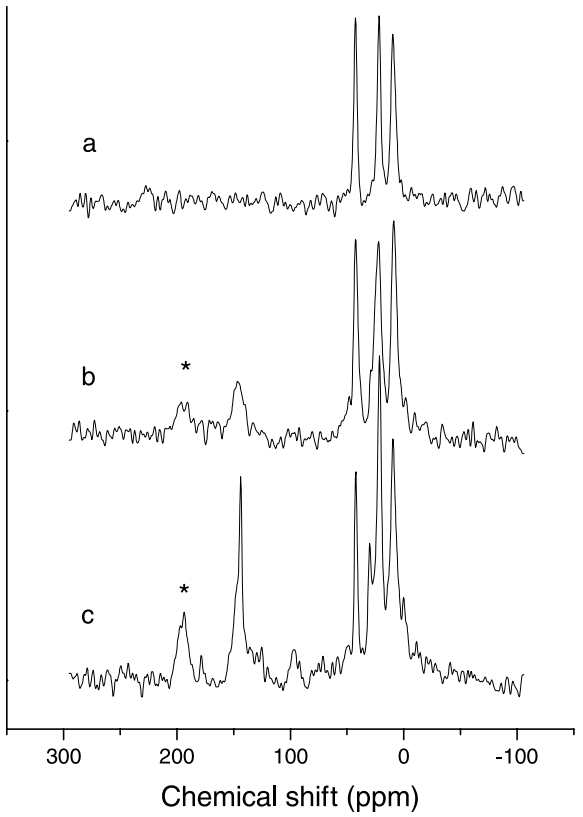

Fig. 5. ^{13}C MAS NMR spectra of (a) MCM-41–NH_2, (b) MCM-41–NH–C_{60}H solids after multiple washings with toluene, and (c) MCM-41–NH–C_{60}H solids without washing with toluene (∗indicates the sideband of the peak at $\delta = 147$ ppm).

observed the characteristic bands of Ruhemann's purple at 405 and 570 nm for the sample of MCM-41–NH_2 in the presence of ninhydrin (Fig. 4b), which indicates the amino-functional groups are attached to the surface of MCM-41. Fig. 4c shows the intensity of these bands decreases in MCM-41–NH–C_{60}H solids, which indicates that some of the –NH_2 groups are bound with C_{60} and converted to secondary amine, which cannot further react with ninhydrin.

3.2.4. CP/MAS NMR

The $^1H \rightarrow {}^{13}C$ magic angle spinning NMR spectra of MCM-41–NH_2 and MCM-41–NH–C_{60}H solids are shown in Fig. 5a and b, respectively. We observed a new broad peak appears at a chemical shift of 147 ppm, which is assigned to C_{60} bound on the amino group of the surface. It has been reported that fullerene core carbons in HC_{60}–NHR gives rise to a resonance peak at this same frequency [32]. The relatively broader line shape (the full-width half-maximum line width is 12 ppm) indicates very lower mobility of C_{60} in the sample, in contrast with that of free or nearly free C_{60}, e.g. spectrum of neat C_{60} sample gives a line width of 0.06 ppm, and for C_{60} dispersing in the hydrophobic phase of a double hydroxide layer compound exhibits only 0.2 ppm [25]. Furthermore, in the sample *without* multiple washings after the synthesis of MCM-41–NH–C_{60}H, we observed a sharp spike on the top of the relatively broad peak at 147 ppm (Fig. 5c). The spectrum indicates C_{60}^- could distribute both on the outer and inner surface of the nanochannels. Thus, we

infer the observed broad spectral line width at 147 ppm most likely arises from a restricted motion of C_{60} molecules bound to the amino group of the mesoporous materials inside the nanochannels.

3.3. EPR study of C_{60}^-: Evidence of molecular sieving

We performed the following EPR experiments to study the paramagnetic property of C_{60}^- samples in THF solution alone and in the presence of MCM-41–NH_2 solids. The EPR spectrum of the freshly prepared C_{60}^- in THF solution in sealed quartz tubing at 100 K is displayed in Fig. 6a. We observed two spectral features: (1) a broad signal with $g = 1.9970$ and spectral width $\Delta H_{pp} = 27$ G, and (2) a sharp signal with $g = 1.9995$ and $\Delta H_{pp} = 4.4$ G. These spectral features are similar to many of the C_{60}^- spectra reported in the literature [8]. Previously, it has been reported that a common impurity $C_{120}O$ is present in C_{60} solids, mainly resulting from the exposure of C_{60} to air and light [33]. Convincingly, the broad signal has been assigned to C_{60}^- ion, and the sharp one to $C_{120}O^-$ [8,34]. It has been indicated that $C_{120}O$ is easier to undergo one-electron reduction than C_{60}. Thus, even though there is only about 1% $C_{120}O$ present in C_{60} solids [33], if the mixture of C_{60} and $C_{120}O$ does not undergo a complete reduction reaction, the amount of $C_{120}O^-$ could become comparable to that of C_{60}^-. The integrated intensity (total area) ratio of the broad to sharp is about 95 to 5 which indicates that the concentration of C_{60}^- ion about 19 times more than that of $C_{120}O^-$ in the original solution.

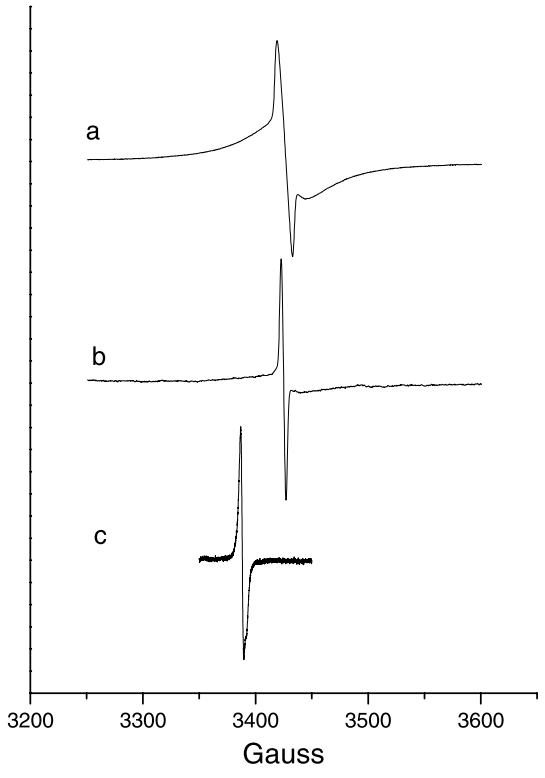

Fig. 6. EPR spectra of: (a) the C_{60}^- samples in THF solution at 100 K, (b) the C_{60}^-/THF solution after the treatment with MCM-41–NH_2 solids (solids were removed before EPR measurements). Note that the broad signal is barely visible, which indicates the molecular sieving property of MCM-41–NH_2 solids, (c) the freshly prepared MCM-41–NH–$C_{60}H$ sample under nitrogen atmosphere.

We further added MCM-41–NH_2 solids to the freshly prepared C_{60}^-/THF samples under a nitrogen atmosphere and examined their EPR spectral features. The EPR spectrum of C_{60}^-/THF solution, after removing MCM-41–NH_2 solids and C_{60} mixture is shown in Fig. 6b. The area ratio of the broad (barely visible) to sharp is about 62 to 38, i.e. 1.6 to 1. Quantitative analysis based on EPR spectra is always difficult, but the relative ratio of these two peaks before (19:1) and after (1.6:1) the addition of MCM-41–NH_2 solids (Fig. 6a and b) infers that MCM-41–NH_2 solids can indeed remove C_{60}^- ion more than $C_{120}O^-$. In other words, MCM-41–NH_2 solids could have molecular sieving property to separate C_{60}^- from $C_{120}O^-$ ions, absorbing the smaller size of C_{60}^- ions, and excluding the bulkier $C_{120}O^-$ ions. This is reasonable on the account of the difference in their molecular size. As described earlier, the nitrogen adsorption study of MCM-41–NH_2 solids gave a pore diameter of 1.7 nm. The diameter of C_{60} and the long axis of $C_{120}O$ (including van der Waals radius) are about 1 and 2 nm, respectively. It is therefore reasonable to expect the $C_{120}O$ molecule would be excluded more from the amino-group modified channel of MCM-41. These EPR studies further confirm that C_{60}^- can be embedded in the channels of MCM-41–NH_2 by the synthetic method as

described earlier. Other detailed EPR studies of free radical attack on C_{60} embedded in the nanochannels of MCM-41–NH_2 solids has been reported elsewhere [16].

We further measured the EPR spectra of the freshly prepared MCM-41–NH–$C_{60}H$ solids under nitrogen atmosphere (Fig. 6c). The signal should correspond to C_{60}^- in the mesoporous solids: $g = 2.0086$ and $\Delta H_{pp} = 2.88$ G. There is an additional shoulder on the high field side of the main peak, which may arise from the anisotropy of C_{60}^- in the solids. Note that the g-value and line width of C_{60}^- in MCM-41–NH–$C_{60}H$ are very different from those of the broad spectra of C_{60}^- (one order of magnitude reduction in line width and an increase in the g-value).

The extraordinary broad signal of C_{60}^- has been attributed to the dynamic Jahn-Teller distortion associated with degeneracy of the ground state [35]. The smaller than the free electron g-value is attributed to spin–orbital coupling effects from unquenched orbital angular momentum [36,37]. However, when C_{60}^- is covalently bound to the amino group in the MCM-41–NH_2 channels, the symmetry of C_{60}^- is greatly reduced. Thus, we observed a drastic change in spectral parameters. Our measured spectral parameters are similar to the reported values obtained in C_{60}^- intercalated in various different zeolites, MCM-41 [38], VPI-15 [17], NaX and NaY [39]. For instance, the EPR parameters of C_{60}^- in MCM-41 with a pore diameter of 1.7 nm were reported as: $g = 2.0024$ and $\Delta H_{pp} = 1.6$ G. Note that the incorporation of C_{60}^- in these mesoporous solids is not through chemical bonding as we have had in our MCM-41–NH–$C_{60}H$ solids.

4. Conclusions

We have demonstrated high concentration of C_{60} can be imbedded in the nanochannels of the amino-modified MCM-41 surface. Very high loading of C_{60} can be further attained using hydrophilic fulleride ions. The physical properties of these modified mesoporous materials were established by various spectroscopic techniques. We further show MCM-41–NH_2 mesoporous materials exhibit molecular sieving property to separate the smaller C_{60}^- from the larger $C_{120}O^-$.

The method we developed for immobilizing C_{60} in the nanochannels of mesoporous silica will allow one to study the chemical reaction of fullerenes in aqueous media. This requires variations in surface functionalization and further pore controls. Future developments to control pore size, surface structure and ligand variations are currently undertaken.

Acknowledgements

This work was supported by grants from the Ministry of Education through Academy Excellent program and Chinese Petroleum Company, Taiwan and NSC International program (NSC 90-2113-M-002-057). T.-S. Lin would like to acknowledge a Visiting Professorship award from NSC of Taiwan during his sabbatical leave at NTU (Spring, 2000), and a partial support by a grant from NSF-International program (NSF# 0115082). We would like to thank Mr. Liu Li-Jung for assistance in the preparation of some samples.

References

[1] J.S. Beck, J.C. Vartuli, W.J. Roth, M.E. Leonowicz, C.T. Kresge, K.D.C. Schmitt, T.-W. Chu, D.H. Olson, E.W. Sheppard, S.B. Higgins, J.L. Schlenker, J. Am. Chem. Soc. 114 (1992) 10834.
[2] C.T. Kresge, M.E. Leonowicz, W.J. Roth, J.C. Vartuli, J.S. Beck, Nature 359 (1992) 710.
[3] H.-P. Lin, Y.-R. Cheng, C.-R. Lin, F.-Y. Li, C.-L. Chen, S.-T. Wong, S. Cheng, S.-B. Liu, B.-Z. Wan, C.-Y. Mou, C.-Y. Tang, C.-Y. Lin, J. Chin. Chem. Soc. 46 (1999) 495.
[4] C.J. Liu, S.G. Li, W.Q. Pang, C.M. Che, Chem. Commun. (1997) 65.
[5] X. Feng, G.E. Fryxell, L.Q. Wang, A.Y. Kim, J. Liu, Science 276 (1997) 923.
[6] M. Antonietti, K. Landfester, Y. Mastai, Israel J. Chem. 41 (2001) 1.
[7] N.J. Turro, Acc. Chem. Res. 33 (2000) 637.
[8] C.A. Reed, R.D. Bolskar, Chem. Rev. 100 (2000) 1075.
[9] P.J. Krusic, E. Wasserman, P.N. Keizer, J.R. Morton, K.F. Preston, Science 254 (1991) 1183;
P.J. Krusic, E. Wasserman, B.A. Parkinson, B. Malone, E.R. Holler, P.N. Keizer, J.R. Morton, K.F. Preston, J. Am. Chem. Soc. 113 (1991) 274.

[10] L.L. Dugan, D.M. Turetsky, C. Du, D. Lobner, M. Sheeler, R. Almli, C.K.-F. Shen, T.-Y. Luh, D.W. Choi, T.-S. Lin, Proc. Nat. Acad. Sci. 94 (1997) 9434.
[11] G. Gu, W. Ding, Y. Du, H. Huang, S. Yang, Appl. Phys. Lett. 70 (1997) 2619.
[12] O.-H. Kwon, H. Yoo, K. Park, B. Tu, R. Ryoo, D.-J. Jang, J. Phys. Chem. B 105 (2001) 4195.
[13] F. Rachdi, L. Hajji, C. Goze, D.J. Jones, P. Maireles-Torres, J. Roziere, Solid State Commun. 100 (1996) 237.
[14] A. Govindaraj, M. Nath, M. Eswaramoorthy, Chem. Phys. Lett. 317 (2000) 35.
[15] I. Piwonski, J. Zajac, D.J. Jones, J. Roziere, S. Partyka, S. Plaza, Langmuir 16 (2000) 9488.
[16] C.-H. Lee, T.-S. Lin, C.-Y. Mou, Phys. Chem. Chem. Phys. 13 (2002) 3106.
[17] O.H. Kwon, K. Park, D.J. Jang, Chem. Phys. Lett. 346 (2001) 195.
[18] A. Hirsh, Q. Li, F. Wudl, Angw. Chem. Int. Ed., Eng. 30 (1991) 1309.
[19] A. Skiebe, A. Hirsh, H. Klos, B. Gotschy, Chem. Phys. Lett. 220 (1994) 138.
[20] D.S. Shephard, W. Zhou, T. Maschmeyer, J.M. Matters, C.L. Roper, S. Parsons, B.F.G. Johnson, M.J. Duer, Angw. Chem. Int. Ed. 37 (1998) 2719.
[21] S. Pekker, L. Ferro, L.L. Mihaly, A. Janossy, Solid State Commun. 90 (1994) 349.
[22] A. Honnerscheid, L. Van Wullen, M.J. Jansen, Chem. Phys. 115 (2001) 7161.
[23] P. Boulas, R. Subramanian, W. Kutner, M.T. Jones, K.M. Kadish, J. Electrochem. Soc. 140 (1993) L130.
[24] J. Stinchcombe, A. Penicaud, P. Bhyrappa, P.D.W. Boyd, C.A. Reed, J. Am. Chem. Soc. 115 (1993) 5212, 116 (1994) 6484.
[25] W. Tseng, J. Lin, C.-Y. Mou, S. Cheng, S.-B. Liu, P.P. Chu, H.-W. Liu, J. Am. Chem. Soc. 118 (1996) 4411.
[26] D.L. Pavia, G.M. Lampman, G.S. Kriz, Introduction to Spectroscopy, second ed., Saunders College Publishing, 1996, p. 75.
[27] J. Chen, Q. Li, H. Ding, W. Pang, R. Xu, Langmuir 13 (1997) 2050.
[28] J. Evans, A.B. Zaki, M.Y. El-Sheikh, S.A. El-Safty, J. Phys. Chem. B 104 (2000) 10271.
[29] (a) M. Ozawa, J. Li, K. Nakahara, L. Xiao, H. Sugawara, K. Kitazawa, K. Kinbara, K.J. Saigo, J. Polym. Sci. 36 (1998) 3139;
(b) L. Lamparth, A.J. Hirsh, Chem. Soc. Chem. Commun. (1994) 1727.
[30] S.Y. Choi, Y.J. Lee, Y.S. Park, K. Ha, K.B. Yoon, J. Am. Chem. Soc. 122 (2000) 5201.
[31] (a) S. Sheng, J.J. Kraft, S.M. Schuster, Anal. Biochem. 211 (1993) 242;
(b) M.M. Joullie, T.R. Thompson, N.H. Nemeroff, Tetrahedron 47 (1991) 8791;
(c) M. Friedman, C.W. Sigel, Biochem. 5 (1996) 478.
[32] X. Wei, C. Hu, Z. Suo, P. Wang, W. Zhang, Z. Xu, E.C. Alyea, Chem. Phys. Lett. 300 (1999) 385.
[33] R. Taylor, M.P. Barrow, T.J. Drewello, Chem. Soc. Chem. Commun. (1998) 2497.
[34] P. Paul, R.D. Bolskar, A.M. Clark, C.A. Reed, Chem. Commun. (2000) 1229.
[35] D. Dubois, M.T. Jones, K.M. Kadish, J. Am. Chem. Soc. 114 (1992) 6446.
[36] T. Kato, T. Kodama, M. Oyama, S. Shida, T. Nakagawa, Y. Matasu, S. Suzuki, H. Shiromaru, K. Yamauchi, Y. Achiba, Chem. Phys. Lett. 186 (1991) 35.
[37] T. Kato, T. Kodma, T. Shida, Chem. Phys. Lett. 205 (1993) 405.
[38] F. Rachdi, L. Hajji, C. Goze, D.J. Jones, P. Maireles-Torres, J. Roziere, Solid State Commun. 100 (1996) 237.
[39] O.-H. Kwon, H. Yoo, D.-J. Jang, Eur. Phys. J. D. 18 (2002) 69.